9-2002

Solution and Micelle-Bound Structures of Tachyplesin I and Its Active Aromatic Linear Derivatives

Alain Laederach
Iowa State University

Amy H. Andreotti
Iowa State University, amyand@iastate.edu

D. Bruce Fulton
Iowa State University, bfulton@iastate.edu

Solution and Micelle-Bound Structures of Tachyplesin I and Its Active Aromatic Linear Derivatives

Abstract

Tachyplesin I is a 17-residue peptide isolated from the horseshoe crab, *Tachyplesus tridentatus.* It has high antimicrobial activity and adopts a β-hairpin conformation in solution stabilized by two cross-strand disulfide bonds. We report an NMR structural investigation of wild-type tachyplesin I and three linear derivatives (denoted TPY4, TPF4, and TPA4 in which the bridging cysteine residues are uniformly replaced with tyrosine, phenylalanine, and alanine, respectively). The three-dimensional aqueous solution structures of the wild type and the active variant TPY4 reveal very similar β-hairpin conformations. In contrast, the inactive variant TPA4 is unstructured in solution. The arrangement of the tyrosine side chains in the TPY4 structure suggests that the β-hairpin is stabilized by aromatic ring stacking interactions. This is supported by experiments in which the β-hairpin structure of TPF4 is disrupted by the addition of phenol, but not by the addition of an equimolar amount of cyclohexanol. We have also determined the structures of wild-type tachyplesin I and TPY4 in the presence of dodecylphosphocholine micelles. Both peptides undergo significant conformational rearrangement upon micelle association. Analysis of the micelle-associated peptide structures shows an increased level of exposure of specific hydrophobic side chains and an increased hydrophobic integy moment. Comparison of the structures in micelle and aqueous solution for both wild-type tachyplesin I and TPY4 reveals two requirements for high antimicrobial activity: a β-hairpin fold in solution and the ability to rearrange critical side chain residues upon membrane association.

Disciplines

Biochemistry, Biophysics, and Structural Biology | Molecular Biology

Comments

Reprinted (adapted) with permission from *Biochemistry* 41 (2002): 12359, doi:10.1021/bi026185z.

Solution and Micelle-Bound Structures of Tachyplesin I and Its Active Aromatic Linear Derivatives[†,‡]

Alain Laederach,[§,||] Amy H. Andreotti,[§,⊥] and D. Bruce Fulton*[,⊥]

Department of Biochemistry, Biophysics and Molecular Biology, Program of Bioinformatics and Computational Biology, and Department of Chemical Engineering, Iowa State University, Ames, Iowa 50011

Received May 23, 2002; Revised Manuscript Received August 17, 2002

ABSTRACT: Tachyplesin I is a 17-residue peptide isolated from the horseshoe crab, *Tachyplesus tridentatus.* It has high antimicrobial activity and adopts a β-hairpin conformation in solution stabilized by two cross-strand disulfide bonds. We report an NMR structural investigation of wild-type tachyplesin I and three linear derivatives (denoted TPY4, TPF4, and TPA4 in which the bridging cysteine residues are uniformly replaced with tyrosine, phenylalanine, and alanine, respectively). The three-dimensional aqueous solution structures of the wild type and the active variant TPY4 reveal very similar β-hairpin conformations. In contrast, the inactive variant TPA4 is unstructured in solution. The arrangement of the tyrosine side chains in the TPY4 structure suggests that the β-hairpin is stabilized by aromatic ring stacking interactions. This is supported by experiments in which the β-hairpin structure of TPF4 is disrupted by the addition of phenol, but not by the addition of an equimolar amount of cyclohexanol. We have also determined the structures of wild-type tachyplesin I and TPY4 in the presence of dodecylphosphocholine micelles. Both peptides undergo significant conformational rearrangement upon micelle association. Analysis of the micelle-associated peptide structures shows an increased level of exposure of specific hydrophobic side chains and an increased hydrophobic integy moment. Comparison of the structures in micelle and aqueous solution for both wild-type tachyplesin I and TPY4 reveals two requirements for high antimicrobial activity: a β-hairpin fold in solution and the ability to rearrange critical side chain residues upon membrane association.

Cationic antimicrobial peptides are produced by many organisms as components of the host defense system (*1*). A typical example is tachyplesin I (Figure 1a), a 17-residue cyclic peptide isolated from the hemocytes of the horseshoe crab, *Tachyplesus tridentatus* (*2*), which is active against fungi and Gram-positive and Gram-negative bacteria (*3*). In aqueous solution, tachyplesin I adopts a β-hairpin fold stabilized by two disulfide bridges (*4*, *5*). Antimicrobial activity is greatly decreased when the four cysteine residues are alkylated or mutated to alanine (TPA4,[1] Figure 1a) (*3*, *6*, *7*), suggesting that the two disulfide bridges are necessary for activity. However, a recent comprehensive mutagenesis study (*7*) has shown that replacement of the four cysteine residues with tyrosine or phenylalanine (TPY4 or TPF4, respectively, Figure 1a) actually increased antimicrobial activity against *Aspergillus flavus*, *Fusarium graminearum*, *Fusarium moniliforme*, and *Escherichia coli*. The CD spectra of both of the aromatic derivatives (TPY4 and TPF4) resembled those of wild-type tachyplesin I (*7*) in aqueous solution. In contrast, the CD spectra of hydrophobic (Cys replaced with Ile, Leu, Val, and Ala) or acidic (Asp) derivatives differed significantly from those of the wild type. Antimicrobial activity for these variants was also lower than that of the wild type, TPY4, or TPF4 (*7*).

There is considerable interest in how the structure of antimicrobial peptides is related to their activity (*8*, *9*). Wild-type tachyplesin I and its active linear derivatives (TPY4 and TPF4) present a unique system for understanding this relationship. Given the wide range of peptide conformations that exhibit antimicrobial activity (helical, β-sheet, and random coil), it is clear that a specific conformation is not always a prerequisite for high antimicrobial activity. To better understand the activity−structure relationship, we have structurally characterized wild-type tachyplesin I, TPY4, and TPF4 as well as the inactive variant TPA4 (Figure 1a) in

[†] A.L. is supported by National Science Foundation IGERT Graduate Fellowship 9972653. This work was supported by an Iowa State University SPRIG award to A.H.A.

[‡] The atomic coordinates and corresponding restraints (PDB entries 1MA2, 1MA4, 1MA5, and 1MA6 for wild-type tachyplesin I and TPY4 in solution and tachyplesin I and TPY4 in the presence of DPC micelles, respectively) have been deposited in the Protein Data Bank. Proton chemical shift assignments have been deposited in the BioMagResBank database (entries 5486, 5487, 5488, and 5489 for wild-type tachyplesin I, TPY4, TPF4, and TPA4, respectively).

* To whom correspondence should be addressed: Iowa State University, Ames, IA 50011. E-mail: bfulton@iastate.edu. Phone: (515) 294-2139. Fax: (515) 294-0453.

[§] Program of Bioinformatics and Computational Biology.

[||] Department of Chemical Engineering.

[⊥] Department of Biochemistry, Biophysics and Molecular Biology.

[1] Abbreviations: CD, circular dichroism; DPC, dodecylphosphocholine; NMR, nuclear magnetic resonance; DQF-COSY, double-quantum-filtered correlation spectroscopy; NOE, nuclear Overhauser effect; NOESY, nuclear Overhauser effect spectroscopy; PC, phosphatidylcholine; RET, resonance energy transfer; rmsd, root-mean-square deviation; ROESY, rotating-frame nuclear Overhauser effect spectroscopy; SDS, sodium dodecyl sulfate; TFA, trifluoroacetic acid; TFE, trifluoroethanol; TOCSY, total correlation spectroscopy; TPY4, tyrosine derivative of tachyplesin I; TPF4, phenylalanine derivative of tachyplesin I; TPA4, alanine derivative of tachyplesin I.

10.1021/bi026185z CCC: $22.00
Published on Web 09/17/2002

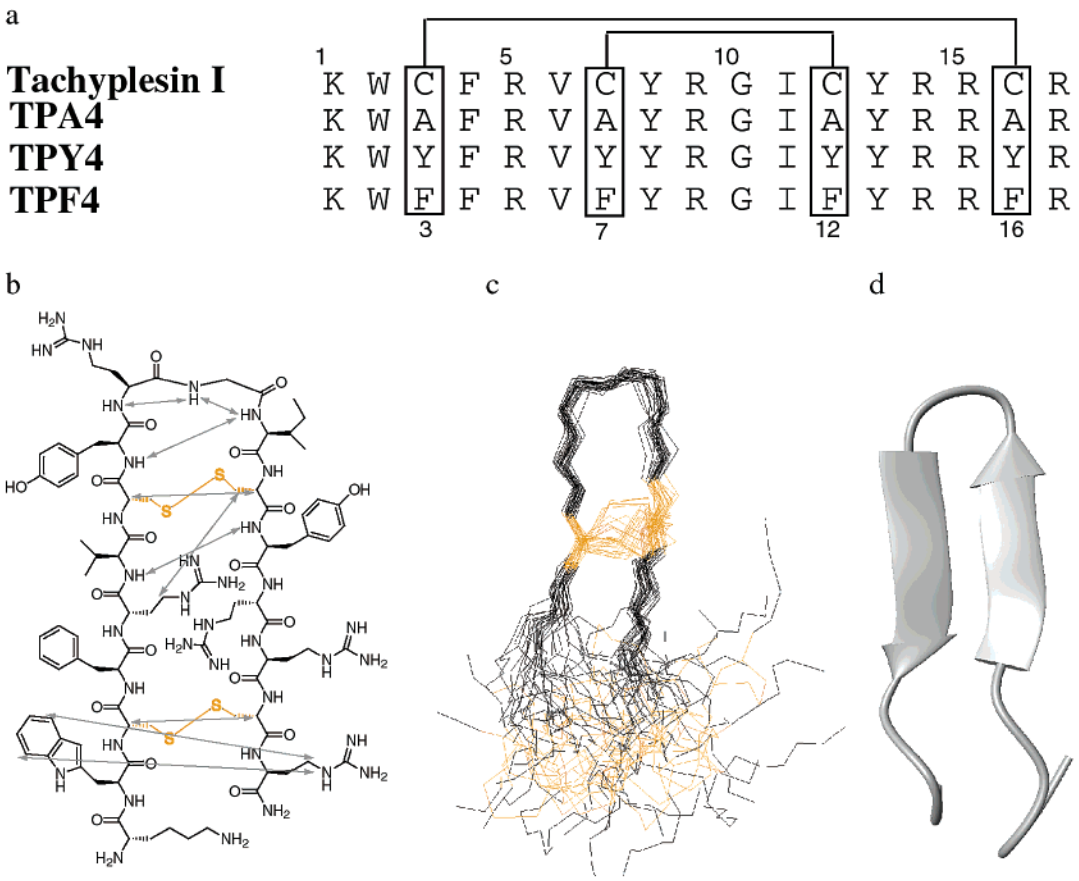

FIGURE 1: (a) Sequences of wild-type tachyplesin I and its linear derivatives, TPY4, TPF4, and TPA4. Disulfide bonds are indicated with lines between Cys3 and Cys16 as well as between Cys7 and Cys12. (b) Schematic representation of wild-type tachyplesin I showing selected nonsequential NOEs as gray arrows. Disulfide bonds and cysteine residues are shown in yellow. (c) Ensemble of 30 solution structures of wild-type tachyplesin I. (d) Minimized average structure of wild-type tachyplesin I in an aqueous environment.

aqueous solution using two-dimensional ^{1}H NMR spectroscopy. TPY4, TPF4, and wild-type tachyplesin I have similar CD spectra and therefore similar secondary structures in aqueous solution (*7*). An NMR structural study will reveal the molecular interactions that stabilize the β-hairpin in TPY4 and TPF4 in the absence of a disulfide bridge.

The activity of tachyplesin I is derived from its ability to permeabilize the cell membranes of pathogens (*9*). It has been proposed that tachyplesin I aggregates within the bilayer and forms anion selective pores (*6*). Thus, a conformational change upon membrane association may play a crucial role in the function of antimicrobial peptides, but the experimental difficulties inherent in studying this change are considerable (*10*). The interior of a detergent micelle reasonably mimics the environment at the interior of a phospholipid bilayer (*11*, *12*). Amphiphilic peptides readily associate with micelles in aqueous buffer and acquire rotational correlation times comparable to those of 20−25 kDa proteins. Micelle-associated peptides therefore are amenable to solution NMR methods (*11*). We determined the structure of wild-type tachyplesin I and TPY4 in the presence of micelles formed by deuterated DPC to better understand the mechanism of membrane permeabilization of tachyplesin I and its active linear derivatives.

MATERIALS AND METHODS

Peptide Synthesis and Purification. Wild-type tachyplesin I was purchased from Bachem (Bubendorf, Switzerland) and used without further purification. All linear derivatives (TPY4, TPF4, and TPA4) of tachyplesin I were synthesized by FMOC-based solid-phase synthesis as described previously (*7*), and purified by reverse-phase HPLC.

NMR Sample Preparation. Peptide concentrations ranged from 0.5 to 1.3 mM in solution and were prepared by dissolving a gravimetrically determined mass of peptide in a 0.15% TFA, 9/1 H_2O/D_2O buffer (pH 3.0). For phenol and cyclohexanol mixing experiments, stock solutions of the deuterated compounds were prepared at 0.83 and 0.35 M in the NMR buffer (pH 3.0); these concentrations correspond to the published maximum solubility of phenol and cyclohexanol in pure water, respectively (*13*). We conducted all mixing experiments at 4 °C, to ensure the highest proportion of structured peptide.

Preparation of a 320 mM stock solution of deuterated DPC (obtained from Cambridge Isotope Laboratories, Andover, MA) was accomplished by dissolving the DPC in the NMR buffer (pH 3.0). A gravimetrically determined mass of the peptide was then dissolved in this stock solution, yielding a concentration of 1.2, 0.6, and 0.5 mM for TPY4, TPA4, and wild-type tachyplesin I, respectively.

NMR Spectroscopy. All NMR spectra were recorded on a Bruker DRX500 spectrometer operating at a ^{1}H frequency of 499.867 MHz. DQF-COSY (*14*), TOCSY (*15*), NOESY (*16*), and ROESY (*17*) spectra were obtained using standard protocols. Spectra were acquired at 4 and 25 °C for aqueous samples and at 40 °C for micelle samples. Proton chemical

shifts were referenced to DSS in identical buffer at the appropriate temperature. All two-dimensional data sets consisted of 1024 × 400−512 complex points. Solvent suppression was achieved using the WATERGATE method (*18*). Mixing times were 90 ms for TOCSY, 100 and 500 ms for NOESY of aqueous samples, 100 ms for NOESY of micelle samples, and 250 and 500 ms for ROESY spectra. The spin-lock field strength was 2.5 kHz for ROESY and 6.4 kHz for TOCSY. DIPSI-2 (*19*) was used for isotropic mixing in TOCSY experiments. Data were processed with Bruker Xwinnmr software and analyzed with NMRView software (*20*).

Temperature coefficients ($\Delta\sigma_{HN}/\Delta T$) were obtained by measuring the chemical shifts of the amide protons for TPY4, TPA4, and TPF4 at 4 and 25 °C and calculating their relative change over that temperature range. Chemical shifts were compared to calculated averages obtained from the BioMagResBank database (*21*) and were determined to be significantly different if they deviated by at least one standard deviation. Peptides lyophilized from water were redissolved in 99% D_2O buffer (pH 3.0) for TPY4 and TPA4, and one-dimensional (1D) spectra were acquired every 10 min for 1 h at 4 °C. The amide region of the spectrum was monitored to determine if any slow exchanging peptides were present.

Structure Calculations. Structure determination was carried out using CNS 1.0 (*22*). NOE restraints were binned according to their integrated volume into three classes, strong (≤2.8 Å), medium (≤3.4 Å), and weak (≤5.0 Å), using the internal calibration utility of NMRView (*20*). The NOE cross-peaks used in structural calculations were verified in the corresponding ROESY spectra by comparing their relative phase to the diagonal to ensure that they did not arise because of spin diffusion (*23*). Due to the lower sensitivity of the ROESY experiment, the corresponding cross-peaks were not present in all cases. Therefore, such cross-peaks (not present in the ROESY) were only used as restraints if they appeared in both the 100 and 500 ms mixing time NOESY spectra. A total of 150−214 NOE restraints were used for the calculation of each structure. The resulting calculated energies are provided in the Supporting Information (Table S7). Three hundred runs of dynamic annealing (*24*) were performed, and the 30 structures with the lowest corresponding total energy were used to compute the minimized average coordinates. MolMol (*25*) was used to overlay the structures and create the molecular illustrations in this paper.

Structural Analysis. Analyses made use of the 30 lowest-energy structures, including the minimized average coordinates. The fraction of side chain accessible surface area was computed for each residue in the 30 structures using the method of Lee and Richards (*26*) as implemented in MolMol (*25*). The average fraction was then calculated for each residue as well as the standard deviation. An unpaired Student's *t* test was applied to each residue to determine if the fraction of accessible surface area was significantly different in the micelle-bound and solution conformers at the 99% confidence interval. VolSurf (*27*) was used to compute the hydrophobic integy moments at two different interaction energies (−0.4 and −0.8 kcal/mol) using both the wild-type tachyplesin I and TPY4 minimized average structures in solution and in the presence of DPC micelles.

RESULTS

Assignment of Two-Dimensional (2D) ^1H NMR Spectra for Wild-Type Tachyplesin I, TPY4, TPF4, and TPA4. For wild-type tachyplesin I, TPY4, TPF4, and TPA4, proton resonance frequency assignments were obtained using standard protocols and are reported in the Supporting Information (Tables S1−S6) (*28*). The observed proton resonance frequencies for wild-type tachyplesin I were nearly identical to those previously reported (*4*, *5*). For both TPF4 and TPY4, it was possible to unambiguously assign backbone amide and α proton resonance frequencies for the entire peptide. All side chain proton resonance frequencies were assigned for TPY4. Complete assignment of the aromatic proton frequencies was not possible for TPF4 due to spectral overlap. The frequencies for TPA4 were poorly dispersed and resembled those for a random coil peptide. In particular, the TPA4 backbone proton frequencies for residues Arg14, Arg15, Ala16, and Arg17 overlapped significantly and were not assigned. Shifts differing significantly from database average values (shown in bold in Tables S1−S6) included the α- and *β* protons of the disulfide-bonded cysteine residues in wild-type tachyplesin I, as well as the Arg9 α proton in the wild type, TPY4, and TPF4. The shifts of the cysteine α and *β* protons in the wild type are typical for such protons in disulfide linkages (*29*). The upfield shift of the Arg9 α proton is likely due to its location at the $i + 2$ (*28*) position of a type I *β*-turn. In contrast, the chemical shift of the Arg9 α proton in TPA4 falls within the expected range, indicating it is likely not within a turn.

In the presence of DPC micelles, both wild-type tachyplesin I and TPY4 exhibited sufficient chemical shift dispersion, allowing unambiguous assignment of most proton frequencies, including all aromatic frequencies in TPY4. As before, the cysteine α and *β* proton resonance frequencies for wild-type tachyplesin I deviated from average values due to the disulfide bridge and the Arg9 Hα proton was shifted upfield due to the *β*-turn. Interestingly, both Arg5 and Arg14 Hα protons were shifted downfield compared to their positions in water. In TPY4, the Arg9 Hα proton chemical shift was within the expected range, but Val6 HN and Hα were both shifted upfield (Supporting Information Tables S4−S6). These changes in chemical shift are consistent with a conformational change of the peptide in the presence of micelles.

Determination of the Structure of Wild-Type Tachyplesin I in Water. Cross-strand NOE cross-peaks observed for wild-type tachyplesin I are schematically represented in Figure 1b, and include all those reported previously by Tamamura et al. (*5*). In addition, we found NOE cross-peaks from the Trp2 Hζ3 and Trp2 Hε3 protons to the Arg17 H*γ* protons. These NOE distance restraints as well as hydrogen bond constraints reported previously (*5*) were used to determine the ensemble of wild-type tachyplesin I structures shown in Figure 1c. The minimized average structure is an antiparallel *β*-hairpin stabilized by two disulfide bridges from Cys3 to Cys16 and from Cys7 to Cys12 (Figure 1d), with residues Tyr8−Ile11 forming a type I *β*-turn. The backbone atom rmsd for residues 4−14 is 0.85 ± 0.11 Å.

Determination of the Structure of TPY4 in Water. The NMR line widths for TPY4 were invariant over the concentration range 0.01−1 mM, indicating that it is monomeric under the conditions used in this study. NOE restraints

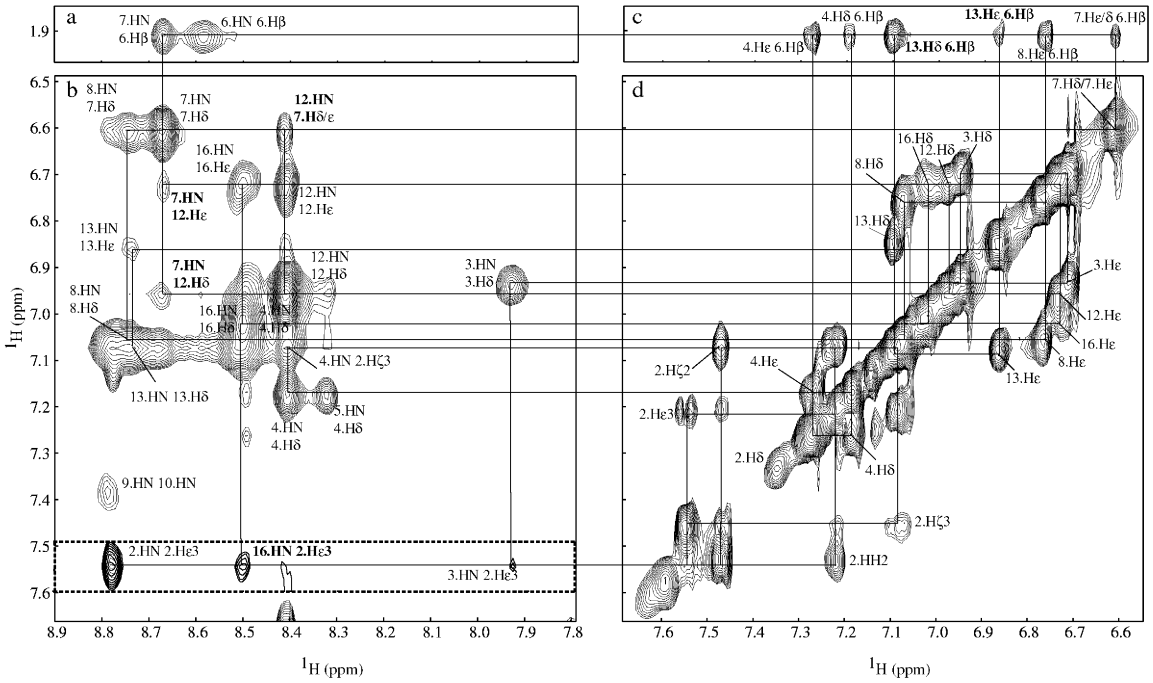

FIGURE 2: 2D ^{1}H NMR spectra of TPY4 at 4 °C. Cross-strand NOE cross-peaks mentioned in the text are indicated in bold type. (a) NOESY in water, (b) NOESY in water (portion of spectrum at the lower contour level denoted with a dashed line is shown for clarity), (c) NOESY in D_2O, and (d) TOCSY in D_2O. For all NOESY data, $t_{mix} = 500$ ms.

obtained from spectra acquired at 4 °C were used to determine the three-dimensional structure of TPY4. The good dispersion in the aromatic region at 4 °C (Figure 2d) allowed unambiguous identification of NOEs from the Hδ and Hϵ protons of Tyr13 to the Val6 Hβ protons (Figure 2a,c) and from the amide protons of Tyr7 to the aromatic protons of Tyr12 (Figure 2b). A weak cross-strand NOE from the Tyr16 HN proton to the Trp2 Hϵ3 proton (Figure 2b inset) indicates that the amino and carboxy termini are close together. Cross-strand NOEs observed for TPY4 correspond to NOEs involving equivalent residues in wild-type tachyplesin I (Figures 1b and 3a). TPY4, therefore, also appears to adopt a β-hairpin conformation with a type I β-turn starting at residue Tyr8. This is consistent with the observation that the CD spectra in water of TPY4 and wild-type tachyplesin I are nearly identical (*7*).

No amide protons in TPY4 (with the exception of Ile11 HN) exhibited a reduced chemical shift temperature coefficient (Supporting Information Figure F2). Although the reduced temperature coefficient of Ile11 HN may be due to a hydrogen bond to the Tyr8 carboxyl, the presence of a neighboring aromatic residue (Tyr12) could also contribute to the reduced coefficient due to temperature-dependent anisotropic deshielding (*30*). Furthermore, no slowly exchanging amide protons were identified when the lyophilized peptide was dissolved in D_2O. Therefore, hydrogen bond restraints were not used in the structural calculations for TPY4.

The 30 lowest-energy structures of TPY4, as determined by successive simulated annealing calculations, are shown in Figure 3b. The backbone atoms of residues 4−14 superimposed to the minimized average structure gave an average backbone rmsd of 0.52 ± 0.12 Å. Figure 3c shows a best fit of the backbone heavy atoms of TPY4 (black) and wild-type tachyplesin I (blue and yellow). The two peptides adopt very similar β-hairpin structures (average backbone rmsd of 2.3 Å). A backbone least-squares fit of the four turn residues (Tyr8−Ile11) of the minimized average structure of wild-type tachyplesin I to that of TPY4 (Figure 3d) gave an rmsd of 0.7 Å.

In Figure 3e, we show the 30 lowest-energy structures of TPY4, including the side chain heavy atoms of Tyr7 and Tyr12. The positions of these side chains are well-defined (heavy atom rmsd of <1.3 Å) due to numerous NOEs between Tyr7 and Tyr12 (Figures 2b and 3a). In the minimized average structure of TPY4 (Figure 3f), the rings of Tyr7 and Tyr12 are parallel with a center−center distance of 3.8 ± 0.7 Å. We propose that stacking of the aromatic rings of Tyr7 and Tyr12, as well as hydrophobic packing of Tyr8 and Tyr13 (ring center distance of 4.4 ± 0.8 Å), is responsible for stabilizing the observed β-hairpin conformation. The NOE observed between Trp2 and Tyr16 suggests that hydrophobic interactions between these two residues may further contribute to stabilization of the TPY4 structure.

NMR Analysis of TPF4 in Water. The 4 °C NOESY spectrum of TPF4 contained several NOEs consistent with a β-hairpin conformation. In particular, characteristic NOEs from Arg9 to Gly10 and from Gly10 to Ile11 indicate that residues 8−11 form a type I β-turn. In general, the assigned cross-peaks formed a subset of the corresponding cross-peaks observed for TPY4. For example, in TPF4 a weak NOE is observed between the Trp2 Hϵ3 and the Hα proton of Arg17, and a medium-intensity NOE exists between the amide protons of Tyr8 and Ile11. We conclude that the aqueous solution structure of TPF4 is similar to that of TPY4.

NMR Analysis of TPA4 in Water. The NOESY spectrum of TPA4 contained strong sequential (i to $i + 1$) α−amide and amide−amide NOEs, while intraresidue NOEs involving side chains were weak and long-range NOEs absent. No evidence for a β-hairpin structure (e.g., Tyr8−Ile11 and

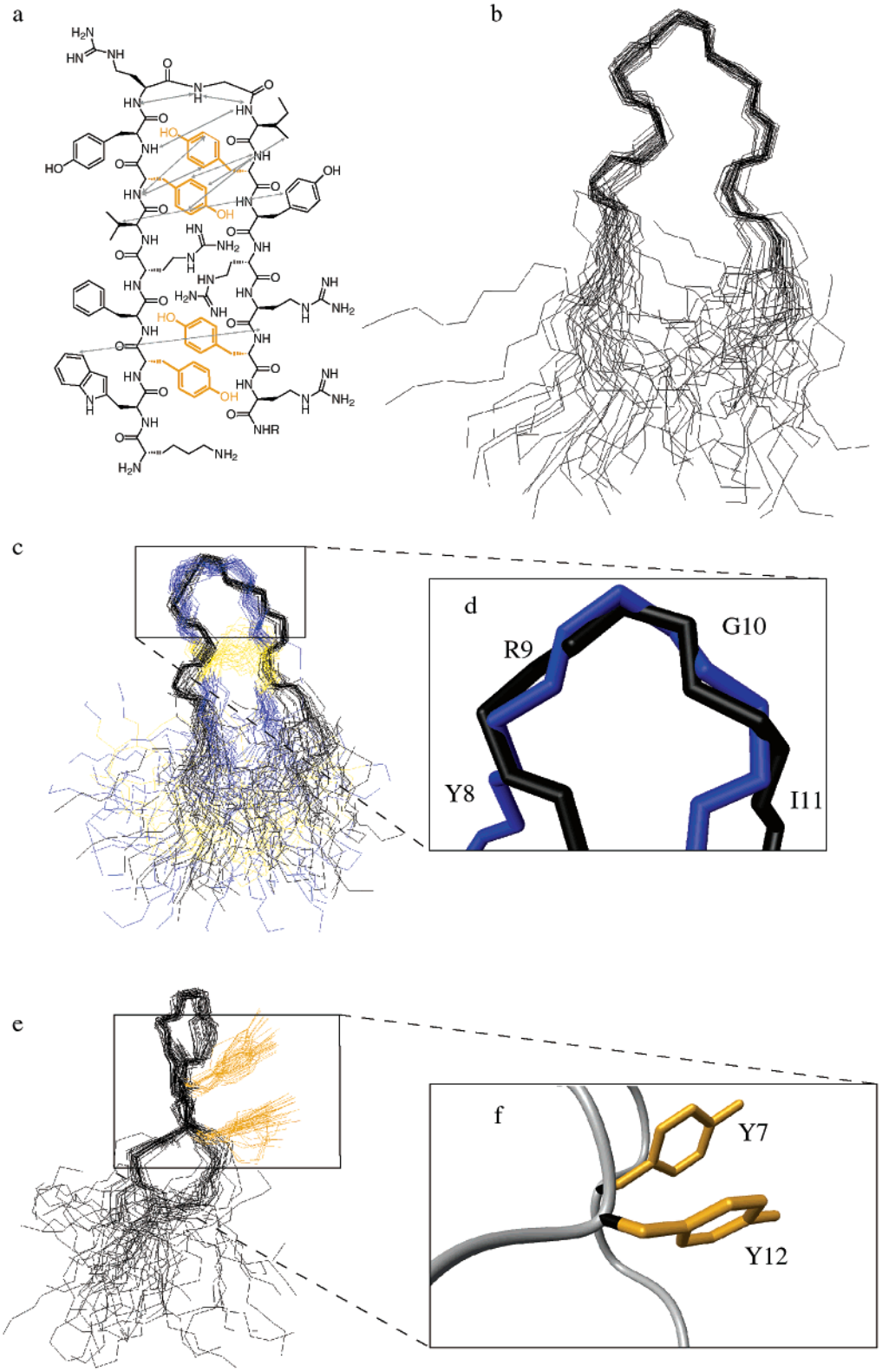

FIGURE 3: (a) TPY4 schematic representation. Selected, nonsequential NOEs are represented as arrows. NOEs observed only at 4 °C are drawn as dotted lines. The four tyrosine residues (Tyr3, Tyr7, Tyr12, and Tyr16) that were mutated from cysteine in wild-type tachyplesin I are shown in yellow. (b) Ensemble of the 30 lowest-energy solution structures of TPY4. (c) Overlay of the 30 low-energy solution structures of TPY4 (black) and wild-type tachyplesin I (blue, with disulfide bonds shown in yellow). (d) overlay of the type I β-turn backbone residues for TPY4 (black) and wild-type tachyplesin I (blue). (e) Ninety-degree rotation of the 30 TPY4 lowest-energy structures shown in panel b, where the Tyr7 and Tyr12 side chain heavy atoms are included in yellow. (f) Minimized average structure of TPY4 showing parallel aromatic stacking of Tyr7 and Tyr12.

Val6−Tyr13 amide−amide NOEs) was observed. Furthermore, chemical shift dispersion was poor, and the shifts resembled those for a random coil peptide. We therefore conclude that the TPA4 derivative is predominantly unstructured in water, in agreement with the reported CD spectrum (*7*).

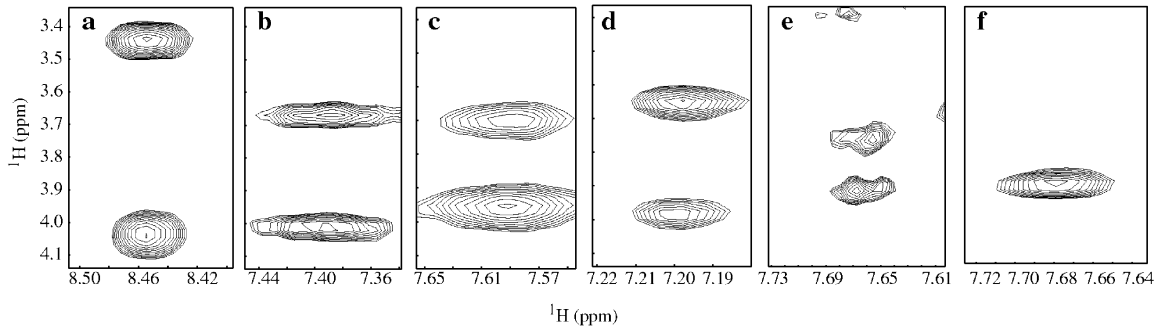

FIGURE 4: Portions of 2D TOCSY or NOESY (t_{mix} = 500 ms) spectra. The peaks correspond to the Gly10 amide to α proton cross-peaks for (a) wild-type tachyplesin I in water, (b) TPY4 in water, (c) TPF4 in water, (d) TPF4 in water and 0.35 M cyclohexanol, (e) TPF4 in water and 0.35 M phenol, and (f) TPA4 in water.

Effect of Phenol and Cyclohexanol on the Conformational Stability of TPF4 and TPY4. Interestingly, the δ and ϵ proton chemical shifts of the four tyrosine residues that replace the cysteine residues in TPY4 (Tyr3, Tyr7, Tyr12, and Tyr16) are shifted upfield compared to the Tyr8 and Tyr13 aromatic protons (Figure 2d). The upfield shift is particularly large for the Tyr7 aromatic protons (0.5 ppm). Yao et al. (*31*, *32*) reported similar upfield shifts of aromatic proton resonance frequencies for residues involved in aromatic ring stacking interactions.

If aromatic ring stacking is indeed responsible for stabilizing the preferred conformation of TPF4 and TPY4, a high concentration of an aromatic molecule such as phenol should destabilize the peptide structure by competitively replacing an aromatic residue at the stacking site. On the other hand, a sterically similar but nonaromatic hydrophobic molecule, such as cyclohexanol, should not disrupt the structure to the same extent. The effect of phenol and cyclohexanol on the stability of the β-hairpin was monitored by a variety of spectral features. NOESY and TOCSY spectra were collected for both TPF4/phenol (at 0.83 and 0.35 M phenol) and TPF4/cyclohexanol (at 0.35 M cyclohexanol) mixtures. Significantly reduced chemical shift dispersion was observed in the spectra of the TPF4/phenol mixture, indicative of diminished conformational stability. We were nonetheless able to assign the amide proton frequencies for residues Trp2−Phe16. Long-range NOE cross-peaks disappeared in the amide−amide region, also consistent with diminished conformational stability. In contrast, the NOESY spectrum of the TPF4/cyclohexanol mixture was nearly identical to that obtained in water alone. All cross-strand NOE cross-peaks were still present, except the weak peak from the Trp2 Hϵ3 to the Hα proton of Arg17, suggesting that cyclohexanol has little effect on the stability of the β-hairpin.

The chemical shift dispersion of the two diastereotopic α protons of Gly10 was used to monitor the degree to which the peptide retained the β-hairpin structure. Figure 4 shows the Gly10 α proton cross-peaks for wild-type tachyplesin I, TPY4, TPF4, and TPA4 under various conditions. For wild-type tachyplesin I (Figure 4a), the chemical shift dispersion of the two Gly10 α protons is large (0.6 ppm), while for both TPY4 and TPF4 in water (panels b and c of Figure 4, respectively), it is somewhat lower (0.3 ppm), but nonetheless indicative of a structured backbone. Upon addition of cyclohexanol, the chemical shift dispersion of these two protons does not change (Figure 4d). However, upon addition of an equimolar amount of phenol (Figure 4e), the cross-peaks coalesce, indicative of a loss of structure. Finally, for the unstructured TPA4 peptide, complete coalescence of the two cross-peaks is observed (Figure 4f).

Structure of Wild-Type Tachyplesin I, TPY4, and TPA4 in the Presence of DPC Micelles. For wild-type tachyplesin I in micelles, all of the cross-strand NOEs observed in water alone were present, with the exception of the NOEs from the Trp2 to the Arg17 side chain protons. Two new long-range NOE cross-peaks appear from the Trp2 HN and Trp2 Hδ1 protons to an Arg9 Hβ proton (Figure 5a). These cross-peaks do not arise from spin diffusion as verified by their sign (negative) relative to the diagonal in a ROESY spectrum (Figure 5a) (*23*). In addition, NOE cross-peaks from the side chain protons of Phe4 to the Val6 β protons and from the ϵ protons of Tyr13 to the β protons of Arg15 also appear. The NOE-restrained structure of wild-type tachyplesin I in the presence of DPC (Figure 5b) is significantly different than that determined in water (Figure 1c). The amino and carboxy termini are folded toward the turn region of the molecule, resulting in a displacement of the two amino-terminal aromatic residues (Trp2 and Phe4) toward Tyr8 and Val6, respectively. The average distance from the Trp2 side chain to the center of the Tyr8 aromatic ring is 7.9 ± 2.0 Å in the micelle-associated structure, whereas the corresponding distance for the peptide in water is 16.0 ± 1.5 Å. This result is consistent with RET experiments (*33*), which reported a reduction of the distance between Trp2 and Tyr8 upon association of wild-type tachyplesin I with PC liposomes. When the two structures are compared, it appears that Arg5 and Arg14 act as hinges that allow conformational rearrangement upon micelle insertion. The Hα chemical shifts for Arg5 and Arg14 are both shifted downfield in micelles, consistent with such a rearrangement (Supporting Information Tables S3 and S4).

A significant conformational change also occurs in TPY4 when it associates with a micelle. NOE cross-peaks from the Trp2 amide proton to the Ile11 Hδ, Ile11 Hβ, and Ile11 Hα (Figure 6a) protons, from the Trp2 Hδ1 to the Ile11 Hβ protons (not shown), and from the Phe4 Hα proton to the Tyr8 Hδ protons indicate that a frame shift occurs in the hairpin. In the NOE-restrained structure (Figure 6b), residues 1−10 are well-ordered (backbone rmsd of 0.65 ± 0.1 Å) and form a hairpin-like structure. The carboxy terminus is largely unstructured, although weak NOE cross-peaks were observed from the δ and ϵ protons of Tyr12 to the α proton of Tyr16. There is a large reduction of the distance between Trp2 and Tyr8 (6.4 ± 2.0 Å in the presence

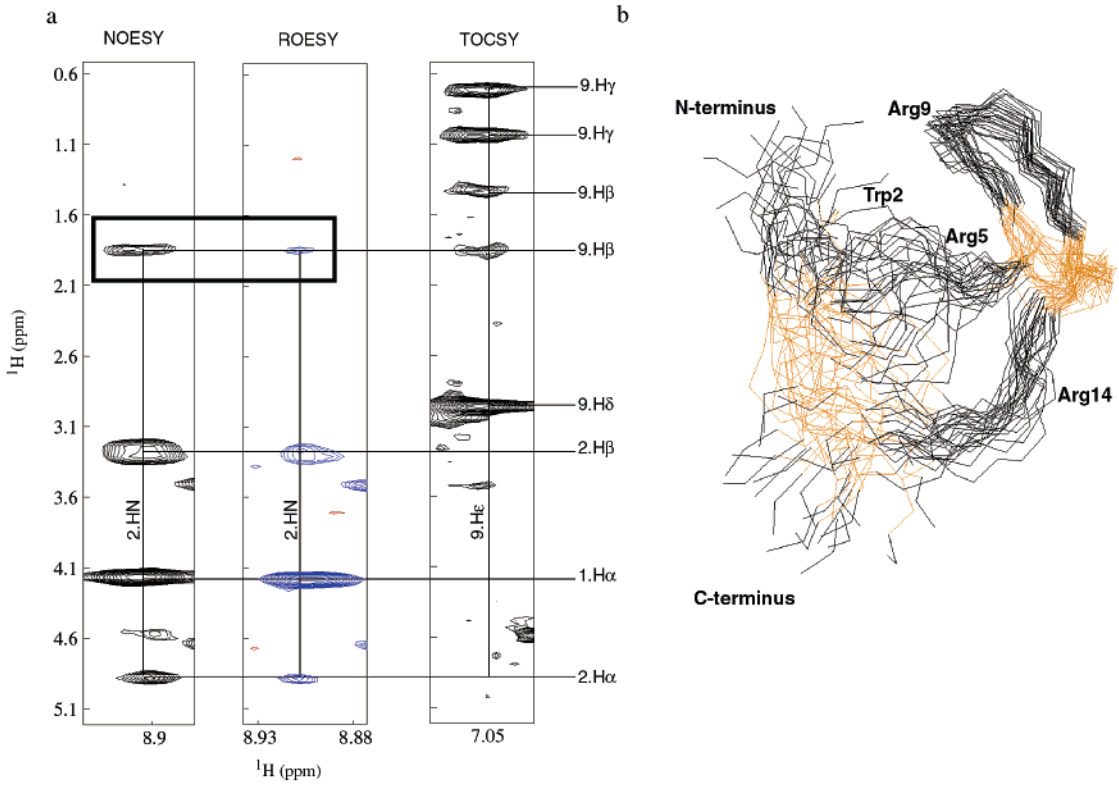

FIGURE 5: (a) Slices of NOESY (t_{mix} = 100 ms), ROESY, and TOCSY spectra at 40 °C of wild-type tachyplesin I in the presence of 320 mM DPC showing an NOE from the Trp2 amide proton to the Arg9 Hβ proton (boxed). The NOE is not a result of spin diffusion because the phase of the corresponding cross-peak is negative in the ROESY spectrum. The positive cross-peaks of the ROESY spectrum are shown in red, while the negative peaks are in blue. (b) Ensemble of minimized structures of wild-type tachyplesin I in the presence of 320 mM DPC; as in Figure 1, the disulfide bonds are shown in yellow.

of DPC compared to 15.2 ± 2.0 Å in solution). There is no NOE evidence that the type I turn spanning residues 8−12 in the solution structure persists in the micelle-associated structure. In fact, the two Gly10 α proton peaks coalesce in the presence of DPC (Supporting Information Figure F1).

When TPA4 was dissolved in the presence of DPC, there was no increase in the dispersion of the backbone amide proton frequencies. Also, few intraresidue and no long-range interresidue NOEs involving side chains were observed. On the basis of these data alone, we cannot exclude the possibility of TPA4 becoming structured in the presence of micelles. It should be noted, however, that Rao observed that TPA4 exhibits a CD spectrum indicative of a random structure in water, 50% TFE, and liposomes (*7*), in agreement with our NMR results. Given the poor chemical shift dispersion and lack of long-range NOEs, we nonetheless conclude that in the presence of DPC micelles the peptide does not adopt a single well-defined conformation.

Analysis of the Structures. The side chain accessible surface area was measured for wild-type tachyplesin I and TPY4 structures in both aqueous and micelle environments. Table 1 lists the residues for which there are significant differences in accessible surface area upon micelle association. Interestingly, for both wild-type tachyplesin I and TPY4, Lys1 has significantly less accessible surface area in micelles than in water, while the opposite is true of Arg17. The conformational rearrangements observed in TPY4 and wild-type tachyplesin I both result in movement of the amino terminus toward the center of the peptide chain, and reduced exposure of the amino-terminal residues. This movement also results in an increased level of exposure of the largely cationic carboxy-terminal residues.

In wild-type tachyplesin I, three hydrophobic side chains (Val6, Tyr8, and Tyr13) are significantly more accessible in the micelle-bound conformation, while only Phe4 is more buried. Similarly for TPY4, four hydrophobic side chains are more exposed (Table 1) while only two are significantly more buried. In general, there is an increase in the hydrophobic accessible surface area of the peptides upon micelle association. The hydrophobic integy moment, which quantifies the amphiphilicity of a molecular structure (*27*), was calculated for the solution and micelle-bound minimized average structures of both TPY4 and wild-type tachyplesin I (Figure 7a). In both cases, the conformational change observed upon micelle association results in increased hydrophobic integy moment norms, indicating that both peptides become more amphiphilic upon micelle association. In both micelle-bound structures (wild-type tachyplesin I and TPY4, panels c and e of Figure 7, respectively), a contiguous, well-defined hydrophobic surface is present, while in the aqueous structures (panels b and d of Figure 7), the polar arginine side chains are interspersed within the hydrophobic surface.

DISCUSSION

Our results indicate that there are two structural requirements for the activity of tachyplesin I and its derivatives: a β-hairpin conformation in aqueous solution and the ability of the peptide to rearrange critical amino acids upon membrane association to increase amphiphilicity. A specific

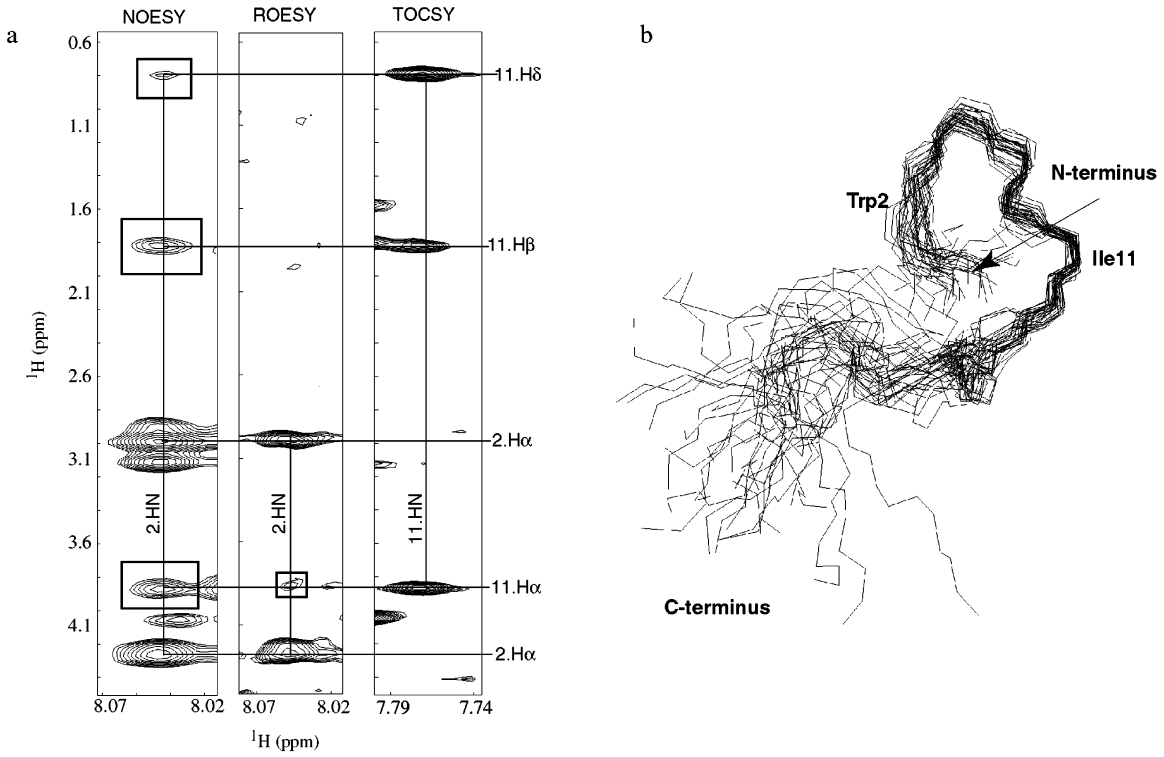

FIGURE 6: (a) Slices of NOESY (t_{mix} = 100 ms), ROESY, and TOCSY spectra for TPY4 in the presence of 320 mM DPC showing NOEs from the Trp2 amide proton to Ile11 Hα and side chain protons. The cross-peak from the Trp2 amide to the Ile11 Hα proton is also present and of negative phase in the ROESY spectrum. However, the two weaker NOEs to the side chain protons of Ile11 are not present in the ROESY spectrum, most likely due to the lower sensitivity of this experiment. For clarity, only the cross-peaks of negative phase are drawn in the ROESY slice. (b) Ensemble of the 30 lowest-energy structures of TPY4 in the presence of 320 mM DPC.

Table 1: Residues with Side Chains that Have Significant Differences (at the 99% confidence interval) in Side Chain Accessibility upon Micelle Association

	residues with side chains that are significantly more accessible upon micelle association	residues with side chains that are significantly less accessible upon micelle association
wild-type tachyplesin I	Val6, Tyr8, Tyr13, Arg14, Arg17	Lys1, Phe4, Arg9
TPY4	Val6, Tyr7, Tyr12, Tyr16, Arg17	Lys1, Trp2, Arg5, Arg9, Ile11

fold in aqueous solution is not a general prerequisite for peptidal antimicrobial activity; the potent antimicrobial peptides leucocin A (*34*), transportan (*35*), and indolicidin (*36*) adopt specific conformations only in the presence of a membrane environment. However, variants of tachyplesin such as TPA4 and TPI4 that do not adopt a β-hairpin conformation in solution have significantly lower antimicrobial activity (*7*). Also, a derivative of tachyplesin in which all four Cys residues are methylated adopts a random coil conformation in solution and exhibits significantly lower activity (*6*). Thus, for tachyplesin I and its variants, the β-hairpin conformation in solution is crucial.

In the aqueous solution structures of tachyplesin I and TPY4, the side chains along the β-hairpin are arranged such that all hydrophobic residues except Trp2 and Phe4 contact another hydrophobic residue across the strand. The total hydrophobic accessible surface area of either of these peptides in the β-hairpin conformation will therefore be smaller than that of a random coil. This has several potential advantages for antimicrobial activity. First, the peptide will have a high water solubility so that it can diffuse to where it is needed. Second, hydrophobic interactions between the peptide and other molecules are reduced in number, inhibiting oligomerization of the peptide while it is in aqueous solution. These first two properties are borne out by the observations that both wild-type tachyplesin I and TPY4 are soluble and monodisperse at concentrations of up to 1 mM. Third, the hydrophobic side chains can be easily transferred through the polar outer portion of the membrane. Finally, another possible advantage of a β-hairpin conformation over random coil is resistance to proteolytic degradation. In fact, tachyplesin I has been reported to be resistant to trypsin digestion (*6*). Defensin, a similar antimicrobial peptide with a disulfide-stabilized β-turn, has been reported to be resistant to proteolysis in the cyclized but not in the reduced form (*37*).

The second structural requirement for activity is the ability to rearrange to a more amphiphilic conformation upon membrane association. This is provided in wild-type tachyplesin by Arg5 and Arg14 which act as hinges. The corresponding rearrangement in TPY4 involves a frame shift of the β-hairpin. Tachyplesin I and TPY4 appear to be structurally adaptive, and their high activity derives from the distinct structures the peptides adopt in solution and in the presence of a membrane.

The antimicrobial activity of peptides is closely related to the composition of the pathogen membrane (*8*). Bacteria and fungi have negatively charged membranes, and the interaction of cationic peptides such as tachyplesin I is mediated in large part by electrostatic interactions. Mammalian cells, on the other hand, have generally neutral cell membranes for which cationic peptides do not have as high an affinity.

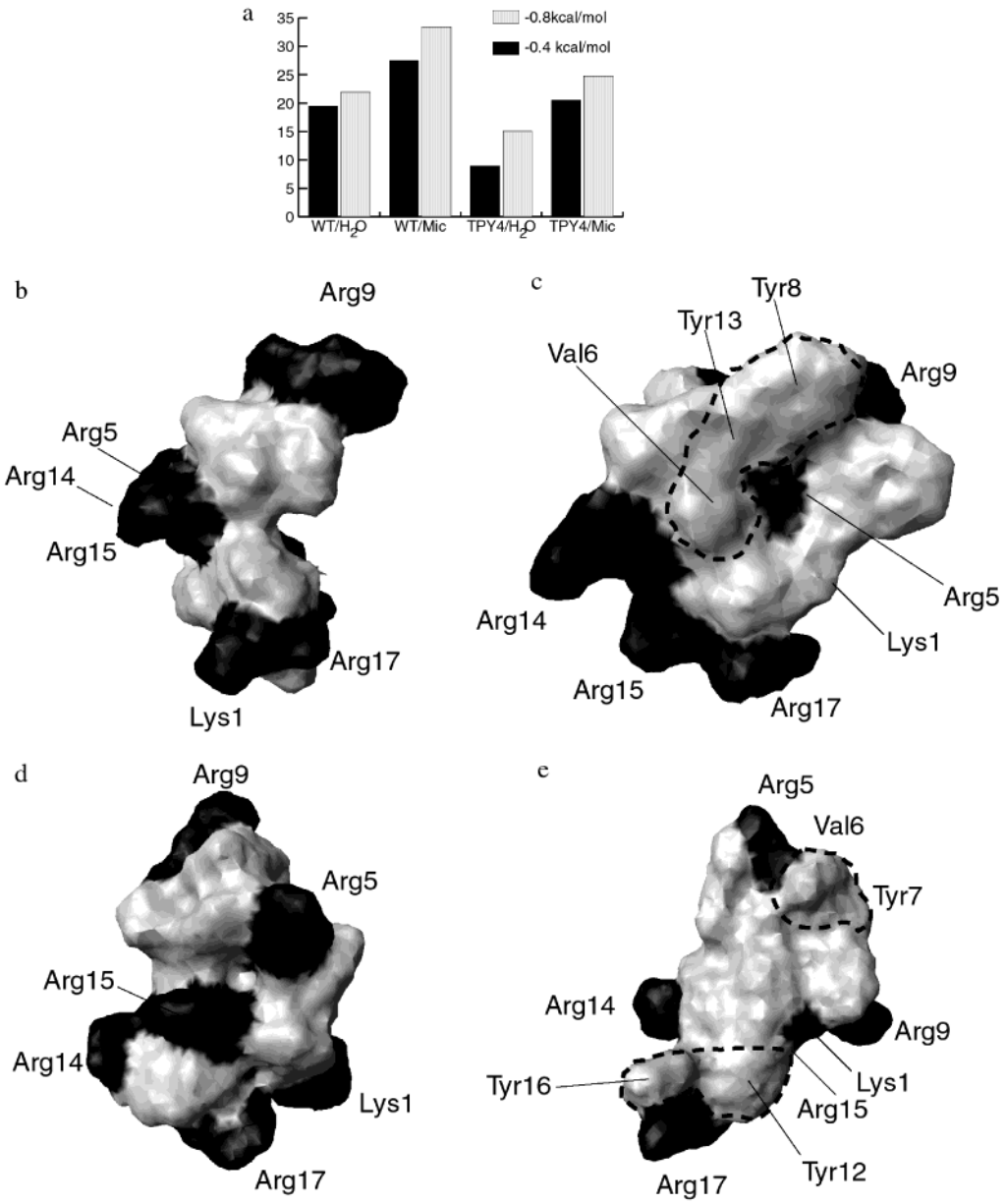

FIGURE 7: (a) Norms of hydrophobic integy moments at the −0.4 and −0.8 kcal/mol energy level for wild-type tachyplesin I (WT) and TPY4 in water (H_2O) and in DPC micelles (Mic). Surface plots of minimized average structures of (b) wild-type tachyplesin I in aqueous solution, (c) wild-type tachyplesin I in the presence of 320 mM DPC, (d) TPY4 in aqueous solution, and (e) TPY4 in the presence of 320 mM DPC. The hydrophobic surfaces are colored in light gray, while the polar surfaces are shown in black. Hydrophobic surfaces that are significantly more solvent-exposed in the micelle-bound conformation, as determined by a Student's *t* test at the 99% confidence interval, are denoted with a dashed line.

We determined structures in the presence of the neutral, zwitterionic detergent DPC. It was not possible to solvate the anionic detergent SDS in the presence of either wild-type tachyplesin I or TPY4 even in a low molar excess (2-fold). Earlier studies have also reported precipitation or turbid solutions when wild-type tachyplesin I was mixed with negatively charged lipids (*5*, *7*, *38*). Certainly, this indicates that ionic interactions may play an important role in the activity of tachyplesins. However, it would be an oversimplification to attribute tachyplesin's antimicrobial activity solely to desolubilization of anionic lipids. The lipid composition of microbial membranes varies, but they generally contain significant fractions of both neutral and anionic lipids (*39*). In such an environment, a complex between tachyplesin and anionic lipid might behave quite differently. There is, in fact, considerable evidence that tachyplesin inserts into and transverses membranes (*6*, *7*, *40*).

Matsuzaki et al. (*6*) have proposed a mechanism for membrane permeabilization by tachyplesin I based upon data from RET experiments on chromophore-labeled vesicles and on cross-membrane conductance measurements on planar bilayers. In their model, tachyplesin I binds to the outer layer of a lipid bilayer without significantly perturbing the membrane, and then self-associates to form anion selective pores. Some of the peptide molecules transverse the bilayer to the inside of the membrane, with a translocation time scale of ∼30 s, and proceed to aggregate and form pores on the inner membrane. The conformational change observed for wild-type tachyplesin I upon association with a micelle is consistent with this mode of action because it results in increased hydrophobicity and amphiphilicity (Figure 7a−e). Increased hydrophobicity allows the peptide to efficiently

traverse the membrane interior. The increased amphiphilicity may orient peptide molecules with respect to the membrane−solvent interface and to each other and thus facilitate pore assembly.

Perhaps the most striking feature of this system is that it is possible to replace four disulfide-linked cysteine residues in an antiparallel β-sheet with tyrosines or phenylalanines, and maintain a very similar fold and antimicrobial activity. Our data (NMR solution structures and disruption of the β-hairpin by phenol but not cyclohexanol) suggest that aromatic ring stacking is responsible for stabilizing the β-turn in TPF4 and TPY4. Stabilization of β-turns by aromatic stacking has been previously observed in short peptides by NMR (*31*, *32*). Replacing disulfide-linked cysteine residues that stabilize β-turns in peptides with aromatic residues may therefore be a viable strategy for the design of linear peptides with specific folds. Such peptides would be expected to retain their fold under reducing conditions that would otherwise cleave disulfide bonds and result in a loss of activity.

ACKNOWLEDGMENT

We thank Dr. A. Gururaj Rao (Pioneer Hibred, Johnston, IA) for providing the TPY4, TPF4, and TPA4 peptides as well as helpful comments and suggestions during the preparation of the manuscript. We also are grateful to Drs. Robert J. Mallis and Ekaterina Pletneva for stimulating discussions during the preparation of the manuscript.

SUPPORTING INFORMATION AVAILABLE

Tables S1−S6 provide proton chemical shift assignments for TPY4, TPF4, TPA4, and wild-type tachyplesin I in solution and wild-type tachyplesin I and TPY4 in the presence of DPC micelles. Table S7 provides energetic details about the structure determination calculation for both wild-type tachyplesin I and TPY4 both in solution and in the presence of micelles. Figure F1 is a portion of the 2D TOCSY spectrum of TPY4 in the presence of 320 mM DPC at 40 °C. Figure F2 reports backbone amide temperature coefficients for TPY4, TPF4, and TPA4. This material is available free of charge via the Internet at http://pubs.acs.org.

REFERENCES

1. Lehrer, R. I., and Ganz, T. (1999) *Curr. Opin. Immunol. 11*, 23−27.
2. Nakamura, T., Furunaka, H., Miyata, T., Tokunaga, F., Muta, T., Iwanaga, S., Niwa, M., Takao, T., and Shimonishi, Y. (1988) *J. Biol. Chem. 263*, 16709−16713.
3. Tamamura, H., Ikoma, R., Niwa, M., Funakoshi, S., Murakami, T., and Fujii, N. (1993) *Chem. Pharm. Bull. 41*, 978−980.
4. Kawano, K., Yoneya, T., Miyata, T., Yoshikawa, K., Tokunaga, F., Terada, Y., and Iwanaga, S. (1990) *J. Biol. Chem. 265*, 15365−15367.
5. Tamamura, H., Kuroda, M., Masuda, M., Otaka, A., Funakoshi, S., Nakashima, H., Yamamoto, N., Waki, M., Matsumoto, A., Lancelin, J. M., Kohda, D., Tate, S., Inagaki, F., and Fiji, N. (1993) *Biochim. Biophys. Acta 1163*, 209−216.
6. Matsuzaki, K., Yoneyama, S., Fujii, N., Miyajima, K., Yamada, K.-i., Kirino, Y., and Anzai, K. (1997) *Biochemistry 36*, 9799−9809.
7. Rao, A. G. (1999) *Arch. Biochem. Biophys. 361*, 127−134.
8. Epand, R. M., and Vogel, H. J. (1999) *Biochim. Biophys. Acta 1462*, 11−28.
9. Matsuzaki, K. (1999) *Biochim. Biophys. Acta 1462*, 1−10.
10. Blondelle, S. E., Lohner, K., and Aguilar, M. (1999) *Biochim. Biophys. Acta 1462*, 89−108.
11. Beswick, V., Guerois, R., Cordier-Ochsenbein, F., Coic, Y. M., Tam, H. D., Tostain, J., Noel, J. P., Sanson, A., and Neumann, J. M. (1999) *Eur. Biophys. J. 28*, 48−58.
12. Kallick, D. A., Tessmer, M. R., Watts, C. R., and Li, C. Y. (1995) *J. Magn. Reson., Ser. B 109*, 60−65.
13. Weast, R. C., and Astle, M. J. (1985) *CRC Handbook of Data on Organic Compounds*, CRC Press, Boca Raton, FL.
14. Piantini, U., Sorensen, O. W., Bodenhausen, G., and Ernst, R. R. (1982) *J. Am. Chem. Soc. 104*, 6800−6802.
15. Braunschweiler, L., and Ernst, R. R. (1983) *J. Magn. Reson. 53*, 521−528.
16. Macura, S., Huang, Y., Suter, D., and Ernst, R. R. (1981) *J. Magn. Reson. 43*, 259−281.
17. Bothner-By, A. A., Stephens, R. L., Lee, J. M., Warren, C. D., and Jeanloz, R. W. (1984) *J. Am. Chem. Soc. 106*, 811−812.
18. Piotto, M., Saudek, V., and Sklenar, V. (1992) *J. Biomol. NMR 2*, 661−665.
19. Shaka, A. J., Lee, C. J., and Pines, A. (1988) *J. Magn. Reson. 77*, 274−293.
20. Johnson, B. A., and Blevins, R. A. (1994) *J. Biomol. NMR 4*, 603−614.
21. Ulrich, E. L., Markley, J. L., and Kyogoku, Y. (1989) *Protein Sequences Data Anal. 2*, 23−37.
22. Brunger, A. T., Adams, P. D., Clore, G. M., DeLano, W. L., Gros, P., Grosse-Kunstleve, R. W., Jiang, J. S., Kuszewski, J., Nilges, M., Pannu, N. S., Read, R. J., Rice, L. M., Simonson, T., and Warren, G. L. (1998) *Acta Crystallogr. D54*, 905−921.
23. Bax, A., Sklenar, V., and Summers, M. F. (1986) *J. Magn. Reson. 70*, 327−333.
24. Nilges, M., Gronenborn, A. M., Brunger, A. T., and Clore, G. M. (1988) *Protein Eng. 2*, 27−38.
25. Koradi, R., Billeter, M., and Wuthrich, K. (1996) *J. Mol. Graphics 14*, 51−55, 29−32.
26. Lee, B., and Richards, F. M. (1971) *J. Mol. Biol. 55*, 379−400.
27. Cruciani, G., Pastor, M., and Guba, W. (2000) *Eur. J. Pharm. Sci. 11*, S29−S39.
28. Wuthrich, K. (1986) *NMR of Proteins and Nucleic Acids*, Wiley, New York.
29. Wuthrich, K. (1976) *NMR in Biological Research: Peptides and Proteins*, North-Holland Publishing Co., Amsterdam.
30. Cierpicki, T., and Otlewski, J. (2001) *J. Biomol. NMR 21*, 249−261.
31. Yao, J., Dysan, H. J., and Wright, P. E. (1994) *J. Mol. Biol. 243*, 754−766.
32. Yao, J., Feher, V. A., Espejo, F., Reymond, M. T., Wright, P. E., and Dysan, H. J. (1994) *J. Mol. Biol. 243*, 736−753.
33. Oishi, O., Yamashita, S., Nishimoto, E., Lee, S., Sugihara, G., and Ohno, M. (1997) *Biochemistry 36*, 4352−4359.
34. Fregeau Gallagher, N. L., Sailer, M., Niemczura, W. P., Nakashima, T. T., Stiles, M. E., and Vederas, J. C. (1997) *Biochemistry 36*, 15062−15072.
35. Lindberg, M., Jarvet, J., Langel, U., and Graslund, A. (2001) *Biochemistry 40*, 3141−3149.
36. Rozek, A., Friedrich, C. L., and Hancock, R. E. (2000) *Biochemistry 39*, 15765−15774.
37. Fujii, G., Selsted, M. E., and Eisenberg, D. (1993) *Protein Sci. 2*, 1301−1312.
38. Oishi, O., Yamashita, S., Lee, S., and Ohno, M. (1993) *Pept. Chem. 31*, 357−360.
39. Lohner, K., and Elmar, J. P. (1999) *Biochim. Biophys. Acta 1462*, 141−156.
40. Matsuzaki, K., Fukui, M., Fujii, N., and Miyajima, K. (1991) *Biochim. Biophys. Acta 1070*, 259−264.

BI026185Z